

Robot-Aided Neurorehabilitation: A Novel Robot for Ankle Rehabilitation

Anindo Roy, *Member, IEEE*, Hermano Igo Krebs, *Senior Member, IEEE*, Dustin J. Williams, Christopher T. Bever, Larry W. Forrester, Richard M. Macko, and Neville Hogan

Abstract—In this paper, we present the design and characterization of a novel ankle robot developed at the Massachusetts Institute of Technology (MIT). This robotic module is being tested with stroke patients at Baltimore Veterans Administration Medical Center. The purpose of the on-going study is to train stroke survivors to overcome common foot drop and balance problems in order to improve their ambulatory performance. Its design follows the same guidelines of our upper extremity designs, i.e., it is a low friction, backdriveable device with intrinsically low mechanical impedance. Here, we report on the design and mechanical characteristics of the robot. We also present data to demonstrate the potential of this device as an efficient clinical measurement tool to estimate intrinsic ankle properties. Given the importance of the ankle during locomotion, an accurate estimate of ankle stiffness would be a valuable asset for locomotor rehabilitation. Our initial ankle stiffness estimates compare favorably with previously published work, indicating that our method may serve as an accurate clinical measurement tool.

Index Terms—Ankle robot, foot drop, neurorehabilitation, rehabilitation robots.

Manuscript received August 6, 2008; revised February 15, 2009. This paper was recommended for publication by Associate Editor E. Gugliemini and Editor K. Lynch upon evaluation of the reviewers' comments. This work was supported in part by the Department of Veterans Affairs Rehabilitation Research and Development Service under Grant B2294T and in part by Baltimore Veterans Affairs Medical Center "Center of Excellence on Task-Oriented Exercise and Robotics in Neurological Diseases" under Grant B3688R.

A. Roy is with the Department of Mechanical Engineering, Massachusetts Institute of Technology, Cambridge, MA 02139 USA, and also with Baltimore Veterans Affairs Medical Center, Baltimore, MD 21201 USA (e-mail: anindo@mit.edu).

H. I. Krebs is with the Department of Mechanical Engineering, Massachusetts Institute of Technology, Cambridge, MA 02139 USA, and with the Department of Neurology and Neuroscience, Burke Medical Research Institute, Weill Medical College, Cornell University, White Plains, NY 10605 USA, and also with the Department of Neurology, University of Maryland School of Medicine, Baltimore, MD 21201 USA (e-mail: hikrebs@mit.edu).

D. J. Williams is with Interactive Motion Technologies, Inc., Cambridge, MA 02138 USA (e-mail: dustinw@interactive-motion.com).

C. T. Bever is with the Department of Neurology and the Veterans Affairs Maryland Health Care System, University of Maryland School of Medicine, Baltimore, MD 21201 USA (e-mail: christopher.bever@va.gov).

L. W. Forrester is with the Department of Physical Therapy and Rehabilitation Science, University of Maryland School of Medicine, Baltimore, MD 21201 USA (e-mail: lforrester@som.umaryland.edu).

R. M. Macko is with the Department of Neurology and Gerontology, Baltimore Veterans Affairs Medical Center, and the Department of Neurology, University of Maryland School of Medicine, Baltimore, MD 21201 USA (e-mail: rmacko@grecc.umaryland.edu).

N. Hogan is with the Department of Mechanical Engineering and the Brain and Cognitive Sciences Department, Massachusetts Institute of Technology, Cambridge, MA 02139 USA (e-mail: neville@mit.edu).

Color versions of one or more of the figures in this paper are available online at <http://ieeexplore.ieee.org>.

Digital Object Identifier 10.1109/TRO.2009.2019783

I. INTRODUCTION

EACH year, over 795 000 Americans suffer a stroke, making it the leading cause of permanent disability in the country [1]. Stroke rehabilitation is a restorative process that seeks to promote recovery, with physical and occupational therapy playing a major role. The motivation behind such therapy is best expressed by Hebbian ideas of nervous system plasticity, mainly that neurons that "fire" together, "wire" together. The human brain is capable of self-reorganization, or neuroplasticity [2], [3], so that learning offers an opportunity for motor recovery [4], [5].

A pioneer of its class, the MIT-MANUS, which is a robotic upper-limb manipulandum for shoulder and elbow training, was completed in 1991 [6]. Clinical trials involving MIT-MANUS have shown that robot-aided neurorehabilitation has a positive impact, reducing impairment during both the subacute and chronic phases of stroke recovery [7]–[14]. This has motivated the development of new modules designed for rehabilitation of antigravity movements, the wrist, the hand, and the ankle [15]. In this paper, we present an overview of the design and characterization of 3-degree-of-freedom (DOF) lower-extremity robotic module developed at MIT, i.e., the ankle robot (Anklebot). We focus on the ankle because it is critical for propulsion during walking and for balance. The ankle is also important in gait for the role it plays in "shock absorption" due to foot placement. Studies have shown that intrinsic ankle properties (e.g., stiffness) are modulated to accommodate surface changes during locomotion.

Following stroke, "drop foot" is a common impairment. It is caused by a weakness in the dorsiflexor muscles that lift the foot. Two major complications of drop foot are slapping of the foot after heel strike (foot slap) and dragging of the toe during swing (toe swing). In addition to inadequate dorsiflexion ("toe-up"), the paretic ankle also suffers from excessive inversion (heel toward midline). This begins in the swing phase and results in toe contact (as opposed to heel contact) and lateral instability in stance. The Anklebot possesses the potential to control both problems since it is actuated in both the sagittal and frontal planes, and our central goal is to determine whether ankle training can improve foot drop in patients with stroke and, possibly, other central lesions, such as cerebral palsy, multiple sclerosis, traumatic brain injury [16], or peripheral nerve pathology.

II. OVERVIEW OF ANKLE TECHNOLOGY

Conventional assistive technology for drop foot includes a mechanical brace called the ankle foot orthosis (AFO) [17].

Although AFOs do offer some biomechanical benefits, there are a number of disadvantages that can be improved [18]. Improvement in assistive technology includes computerized functional electrical stimulation (e.g., WalkAide, Innovative Neurotronics, Inc., Austin, TX; L300, Bioness, Inc., Valencia, CA) and implantable microstimulators (BIONs) to stimulate the deep peroneal nerve and tibialis anterior muscle in order to flex the ankle during swing [19].

Recent advances in therapeutic robotics have led to several devices specific to lower extremity (LE), including those for ankle rehabilitation [16], [19]–[22]. The Lokomat (Hocoma, Zurich, Switzerland) is a widely used LE robot, which is designed as a bilateral computerized gait orthosis used in conjunction with partial body weight support (PBWS) treadmill walking [23]. It mainly guides the hips and knees through preprogrammed kinematics. It does not provide active assistance at the ankle: foot drop is counteracted by a spring-loaded mechanism to support dorsiflexion during the swing phase of gait. Hesse's Gait Trainer I moves the legs in a physiologic way with footplates and has collected so far the largest body of evidence of the impact of LE robotics on stroke recovery (DEGAS [24] and the Cochrane report [25]). Another device is the active AFO (AAFO) [16], which is a novel actuated ankle system placed in parallel with a human ankle that allows dorsi-plantarflexion (DP). The AAFO consists of a series elastic actuator attached posterior to a conventional AFO, and a motor system modulates orthotic joint impedance based on position and force sensory information. Andersen and Sinkjaer [21] developed an ankle joint perturbator that introduces ankle joint rotation to stretch ankle extensors. It provides sufficient dorsiflexion but not plantarflexion torque during gait in addition to limited backdriveability. Another perturbator-type device has been developed by Zhang *et al.* [26]. It stretches the ankle throughout the range of motion (ROM) and evaluates joint stiffness. The "Rutgers Ankle" orthopedic rehabilitation interface is yet another ankle rehabilitation device [22]. It is a Stewart platform-type haptic interface and consists of a computer-controlled robotic platform that measures foot position and orientation. The system uses double-acting pneumatic cylinders, linear potentiometers, and a 6-DOF force sensor. It provides resistive forces and torques on the patient's foot, in response to virtual reality-based exercises. Ferris and colleagues [20] have similarly developed an AFO for the human ankle joint that is powered by artificial pneumatic muscles. This device is able to provide 50% of the peak plantarflexor net muscle moment and about 400% of the peak dorsiflexor net muscle moment during unassisted walking. Finally, Bharadwaj and colleagues developed their robotic gait trainer (RGT) [27] around the same period that we completed MIT's Anklebot. The RGT employs muscle rubber actuators and has a similar tripod layout as MIT's Anklebot [28]. However, contrary to MIT's Anklebot, the RGT has limited ROM in both the sagittal and frontal planes (23° in plantarflexion and 5° in eversion). It is also severely limited by its low maximum operating frequency of 0.5 Hz. The average plantarflexion and inversion of the ankle during toe-off is around 26° (maximum 41°) and 15° (maximum 25°) [29], and human frequency bandwidth can achieve up to 15 Hz. Furthermore, accurate control

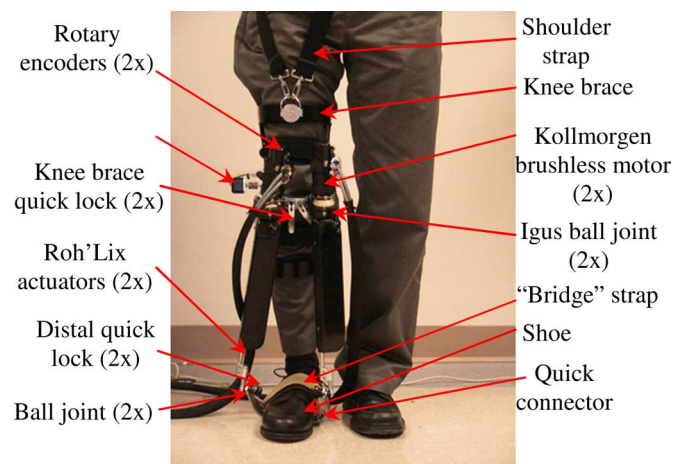


Fig. 1. MIT's ankle robot system. Individual wearing the prototype MIT ankle robot (Anklebot) in standing position. The ankle robot has been designed to deliver therapy in seated, overground, treadmill, and supine positions. Also shown are the different components of the robot.

of impedance might prove to be a clinically important aspect, particularly during gait. While the RGT can produce different impedances, it cannot achieve controllable impedance since any stiffness variation must be always accompanied by a change of force and/or equilibrium, which is not a limitation of the Anklebot. The RGT has no provision to control other important aspects of impedance. For example, there is no way to control the amount of energy that is dissipated during a specified motion. This might be especially important during gait, for example, to prevent the foot from slapping following heel strike.

Here, we describe MIT's Anklebot. We will report on the design choices and the hardware characteristics. We will then demonstrate its potential as a clinical measurement tool in estimating passive ankle properties.

III. DESCRIPTION OF THE ANKLEBOT

A. Hardware

1) *Kinematic Design:* The Anklebot is a 3-DOF wearable robot, backdriveable with low intrinsic mechanical impedance, that weighs less than 3.6 kg. It allows normal ROM in all 3 DOF of the foot relative to the shank during walking overground, on a treadmill, or while sitting (Fig. 1).

The Anklebot provides actuation in two of the ankle's 3 DOF, namely plantar-dorsiflexion and inversion–eversion via two linear actuators mounted in parallel. Internal–external rotation is limited at the ankle with the orientation of the foot in the transverse plane being controlled primarily by rotation of the leg [29]. There is an additional advantage in underactuation, i.e., actuating fewer DOFs than are anatomically present: It allows the device to be installed without requiring precise alignment with the patient's joint axes (ankle and subtalar joints). This is actually an important characteristic of all our robotic devices. In this configuration, if both actuators push or pull in the same direction, a DP torque is produced. Similarly, if the two links push or pull in opposite directions, inversion–eversion torque results. After discarding two benign DOFs, Gruebler's mobility

index is 3, which is same as the mobility of the ankle if modeled as a single joint [28].

The ankle robot allows 25° of dorsiflexion, 45° of plantarflexion, 25° of inversion, 20° of eversion, and 15° of internal or external rotation [14]. These limits are near the maximum range of comfortable motion for normal subjects and beyond what is required for typical gait [29]. The Anklebot can deliver a *continuous net* torque of approximately 23 N·m in DP and 15 N·m in eversion–inversion (IE). It has low friction (0.744 N·m) and inertia (0.8 kg per actuator for a total of 1.6 kg at the foot) to maximize the backdriveability.

Of course, the Anklebot torque capability does not afford lifting the weight of a patient. At best, we can cue the subject to use their voluntary plantarflexor function by providing supplemental support to the paretic ankle plantarflexors during this phase. Therefore, it is important to list our design assumptions. Our design is aimed at affording foot clearance at the end of the stance phase as well as positioning the ankle during swing phase for a controlled landing. Peak dorsiflexion typically occurs in late stance, reaching about 10° prior to toe-off into swing phase. One challenge in gait therapy is how to invoke the sufficient ankle activity to allow about 4° dorsiflexion during late mid-stance [29]. The torque generated by the Anklebot can compensate for drop foot during early and final stance phases of gait and during push-off. We also want to generate torque during the mid-swing phase by adequate concentric activity in the dorsiflexor muscles. In this respect, the Anklebot can provide continuous torques up to ~23 N·m in the sagittal plane, which is higher than required to position the foot in dorsiflexion during mid-swing. Whether our design assumptions were correct remains to be proven in the rehabilitation setting.

2) *Actuation and Transmission*: The Anklebot is actuated by two brushless dc motors (Kollmorgen RBE(H) 00714, Kollmorgen, Northampton, MA), each capable of generating 0.25 N·m¹ *continuous stall*² torque and 0.8 N·m *instantaneous peak* torque (torque constant ~0.07 N·m/A) with a maximum (peak-to-peak) cogging torque of 0.023 N·m and maximum stiction of 0.024 N·m. Each motor weighs 0.391 kg (motor inertia ~ 3.18 × 10⁻⁶ kg·m²), thus possessing a high torque-to-mass ratio (0.637 N·m/kg per motor). Two of these motors produce a *continuous stall* torque of 0.5 N·m (1.6 N·m *peak* torque), which is amplified and transmitted to the foot piece via a pair of parallel linear traction drives (transmission ratio ~35.2). The traction drive consists of two linear screw actuators (Roh'Lix drive, Zero-Max, Inc., Plymouth, MN).

3) *Sensor Technology*: Position information is provided by two sets of sensors: The first set employs Gurley R119 rotary encoders (Gurley, Troy, NY) mounted coaxial with the motors and possessing a resolution of 8.78 × 10⁻³°. The second set

¹Kollmorgen RBE(H) data publication at <http://kollmorgen.com>.

²*Continuous stall torque* (at 25 °C ambient) is the maximum constant torque without rotation resulting in a steady-state winding temperature rise of 130 °C with the standard aluminum heat sink; *peak torque* is the maximum torque available from a given size of motor and is the torque the motor will provide when peak current is provided; *maximum cogging torque* is a torque disturbance based on the magnets in the field attraction to the teeth in the armature; *maximum static friction* is the sum of the retarding torques at start-up or at stall within the motor.

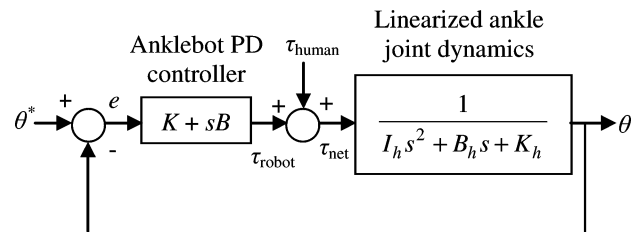


Fig. 2. Schematic representation of the Anklebot control system. In the figure, θ is the ankle angle as measured from neutral, θ^* is the reference ankle angle given to the proportional-derivative (PD) servo, I_h is the moment of inertia of the human ankle, K and K_h are the torsional robot and human ankle stiffness, respectively, B and B_h are the torsional robot and human ankle damping, respectively, and τ is the robot torque acting on the ankle joint.

employs linear incremental encoders (Renishaw, Chicago, IL) with a resolution of 5×10^{-6} m mounted on the traction drive. The rotary encoders are used to commutate the motors. The linear encoders are used as feedback to the controller. The linear dimensions measured by the linear encoders are used to estimate ankle angle in both DOFs. Torque is measured by analog current sensors (Interactive Motion Technologies board employing TI/Burr-Brown INA117P), which provide a measure of motor torque with a nominal resolution of 2.59×10^{-6} N·m.

4) *Controller*: For the passive stiffness measurement included in this paper, we employed a simple impedance controller with a programmable reference position, a programmable proportional gain (approximating a controllable torsional stiffness), and a programmable derivative gain (approximating a controllable torsional damping in parallel with the stiffness), as shown in Fig. 2.

5) *Safety Features*: As with any rehabilitation device, safety is a must. Our failure analysis considered don-on and don-off, body-weight support during gait training, as well as hardware failures. During don-on and don-off, the patient remains seated eliminating any potential for falls. Furthermore, the Anklebot is attached via a set of four quick-release mechanisms plus a snow-board strap with its quick release (see below). In case of emergency, the device can be removed from the patient in less than 30 s. During gait training either on a treadmill or overground, we employ a body-weight support system (LiteGait®, Mobility Research, Tempe, AZ). As an electrically actuated machine capable of independent motion, the device has the potential to injure patients. To minimize the risk, multiple levels of protection were built into the device. All mechanical components were designed with at least four times safety factor. The software continuously monitors torques, velocities, and displacements and disables the system in case preestablished limits are exceeded. Furthermore, the traction drive operates as a mechanical “fuse,” and it slides above preset torque values. An independent electronic circuit monitors in real time the health of the sensors and actuators package. It includes “health-status” signals from the servo amplifiers, Hall-effect sensors, encoders, “heart-beat” signal from the computer, the status of two human-operated “kill switches,” and the status of a “dead-man” switch carried by the therapist during overground or treadmill training. The electrical panel includes a ground fault detector (GFI).

6) *Donning Procedure*: To afford speedy deployment, the patient first dons a pair of shoes and a knee brace, both retrofitted with quick connectors. A top-of-the-line orthopedic knee brace (Townsend Design, Bakersfield, CA) is mounted from the front of the leg (without requiring the foot to be threaded through it). While still seated, the patient's foot is then secured to the robot "foot connection" via a rapid connect–disconnect ("quick-release") mechanism, as well as a single snowboard strap over the bridge of the foot. The strap across the ankle is added not to secure the foot connection but rather to "break" the excessive "synergy" or coupling between the sagittal and frontal plane movements and, in particular, to decrease excessive inversion common among stroke patients. This strap helps minimize potential spastic reaction. In order to avoid interference with the unimpaired leg, the inside of the leg (medial border) is kept free of any obstructions. The robot is then mounted onto the knee brace with the two bicycle-type quick locks with levers. Excluding the time needed to determine the patient's knee brace and shoe sizes, the donning process requires no more than 2 min by a single clinician. Multiple sizes of the knee brace and orthopedic shoe (both for men and women) are available to accommodate individuals with different anthropometric dimensions and for optimal comfort.

7) *Overhead Support for Gait*: A cable festoon system that interfaces with the Anklebot was developed to provide overhead support during overground and treadmill gait. The festoon system consists of two tripod structures and a cable that runs between them. The Anklebot cables connect directly to the festoon cable, and it is passively moved by the therapist or therapist-aide during training so that the patient can walk wearing the robot free of cable interference.

B. Estimation of Ankle Kinematics and Kinetics

To determine the ankle kinematics and torques, we used simple geometry and typical anthropometric data (Fig. 3), sensor outputs, and a simple linearized mathematical model of the shank–ankle–foot system. Ankle angle and torque in the sagittal plane, i.e., DP, are estimated using the following governing relationships:³

$$\begin{aligned} \theta_{dp} &= \sin^{-1}(x) + \theta_{dp, \text{offset}} \\ \tau_{dp} &= (F_{\text{right}} + F_{\text{left}})x_{\text{length}} \\ x &= \left(\frac{x_{\text{tr, len}}^2 + L_{\text{shank}}^2 - x_{\text{link, disp}}^2}{2x_{\text{length}}L_{\text{shank}}} \right) \\ x_{\text{link, disp}} &= \left(\frac{x_{\text{av-act, len}} - x_{\text{right}}}{2} \right) + \left(\frac{x_{\text{av-act, len}} - x_{\text{left}}}{2} \right) \end{aligned} \quad (1)$$

$$(2)$$

where θ_{dp} is the ankle angle as measured from neutral in the sagittal plane, $\theta_{dp, \text{offset}}$ is the offset in ankle angle, τ_{dp} is the

³By convention, angular and linear displacements are assumed positive for dorsiflexion ("toe-up") and eversion ("toe away from midline") and negative for plantarflexion ("toe-down") and inversion ("toe toward midline").

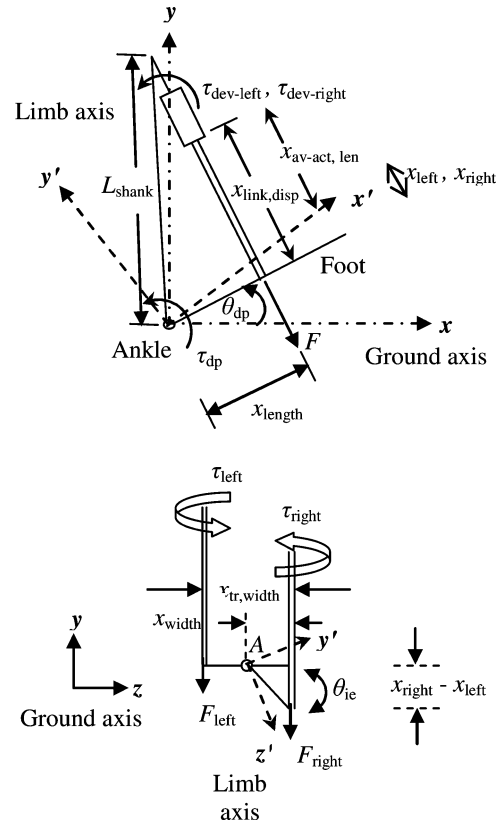


Fig. 3. (Top) Sagittal plane representation of the Anklebot actuators dorsiflexing the human ankle as characterized by relative orientation of the limb axis ($x'-y'$) with respect to the ground axis ($x-y$); (bottom) frontal plane representation with the device evverting (or inverting) the ankle as characterized by relative orientation of the limb axis ($y'-z'$) with respect to the ground axis ($y-z$).

net torque at the ankle joint, F_{right} and F_{left} are the forces generated by the right and left actuators, respectively, x_{length} is the distance between the line of action of actuator force and the point of attachment between the ankle and the robot in the sagittal plane, L_{shank} is the shank length, $x_{\text{link, disp}}$ is the linear displacement of linkage, x_{right} and x_{left} are the lengths of the right and left actuators, respectively, and $x_{\text{av-act, len}}$ is the average actuator length. Ankle angle and torque in the frontal plane i.e., IE, are similarly calculated using link displacement, device geometry, and sensor information

$$\begin{aligned} \theta_{ie} &= \tan^{-1} \left(\frac{x_{\text{right}} - x_{\text{left}}}{x_{\text{tr, width}}} \right) + \theta_{ie, \text{offset}} \\ \tau_{ie} &= (F_{\text{right}} - F_{\text{left}})x_{\text{width}} \end{aligned} \quad (3)$$

where θ_{ie} is the angular displacement from neutral in the frontal plane, $\theta_{ie, \text{offset}}$ is the IE offset angle, $x_{\text{tr, width}}$ is the transverse "ball-to-ball" width, τ_{ie} is the net torque at the ankle joint, and x_{width} is the distance between the line of action of actuator force and the point of attachment between the ankle and robot in the frontal plane (see Fig. 3).

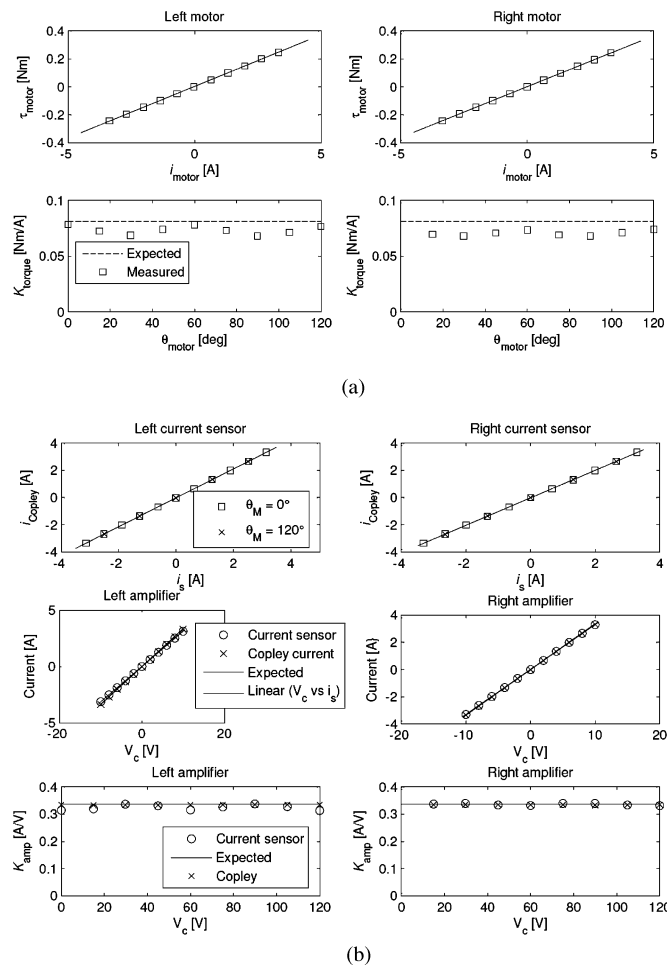


Fig. 4. Characterization of Anklebot actuation package during lock tests. (a) Left and right motor torques (τ_{motor}) versus motor current (i_{motor}) and torque constant (K_{torque}) versus motor position (θ_{motor}). (b) (Top panel) Copley current (i_{Copley}) versus current sensor (i_s) reading for two different motor positions ($\theta_M = 0^\circ, 120^\circ$) shown for both left and right current sensors; (middle panel) behavior of both amplifiers characterized in terms of Copley current, current reading, and expected current each plotted against command voltage (V_c); (bottom panel) variation of amplifier constant (K_{amp}) according to Copley and current sensor measurements against command voltage.

IV. CHARACTERIZATION OF THE ANKLE ROBOT

A. Motors, Servo Amplifiers, and Current Sensors

Characterization of the actuation package during lock tests is shown in Fig. 4. The torque constant of both left and right motors was nearly equal, as seen in Fig. 4(a) (~ 0.07 N-m/A and coefficient of variation $C_v = 0.03$ – 0.05 for motor angle $\theta_M = 0$ – 120°). The behavior of the current sensors was characterized by comparing the measured current against the servo amplifier discrete current update for different motor positions [Fig. 4(b)]. The sensor currents were almost exactly equal to the measured Copley currents ($r^2 = 0.99$, $P \sim 0$) with a negligible bias (-0.02 to -0.013 A) for all motor positions on both sides, thereby validating the accuracy of both the current sensors. Finally, the behavior of the servo amplifiers (Copley Controls, Inc., Montville, NJ) is characterized in terms of their current (command) voltage curves as well as the variability of their

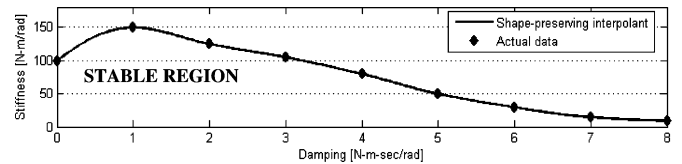


Fig. 5. Impedance characterization and measurement calibration. Impedance ranges of the ankle robot as characterized by the uncoupled stability curve. The graph shows the torsional stiffness versus damping stability profile and the resultant stable region.

(amplifier) constants with respect to changes in motor position [Fig. 4(b)]. We found that the amplifier constants according to both Copley current (0.334 A/V, $C_v = 0.001$) and sensor current (0.324 – 0.335 A/V, $C_v = 0.01$ – 0.02) measurements were relatively invariant to changes in motor position. Further, the current output of the servo amplifiers were a near match to their expected values for both sides, with the error being of the order of only a few milliamperes (0.02 ± 0.01 A).

B. Achievable Impedance

The achievable impedance range of the device is characterized by the uncoupled stability curve shown in Fig. 5. The stability data points were obtained by manually perturbing the Anklebot at the ball joints of the two linear actuators with no user attached to it. This was performed for several values of robot damping, with the highest stiffness attainable determined at each damping value before instability occurred. In this context, instability was characterized by the occurrence of constant nondecaying oscillations. It is important to note that even very “small” oscillations were accounted for in this test. A shape-preserving interpolant was then used to obtain the stability boundary. For proper operation, the controller gains should be chosen below the stability curve.

C. Displacement Validation

In order to verify the accuracy of Anklebot’s estimation of ankle angles, the device was validated by comparison to independent external measurements. To this end, a mock-up of the human ankle was built, and several ramp-and-hold displacements were applied to the mock-up foot [Fig. 6(a)]. We used a mock-up of the shank–ankle–foot to eliminate confounding effects such as placement of the external electrogoniometer and in-shoe slippage.

The resultant angular displacements were compared against angle measurements obtained using a twin-axis electrogoniometer (SG110, Biometrics Ltd., Ladysmith, VA) that simultaneously measures angles in two planes of movement with a maximum error of $\pm 2^\circ$ over a range of $\pm 90^\circ$ [Fig. 7(a)]. The mean absolute error was $\leq 1^\circ$ in both planes of movement (maximum 1.5°). This corresponds to $\leq 2\%$ of the full range of movement measured by the electrogoniometer. To assess repeatability, the validation test was repeated on different days with the setup being completely disassembled and reassembled to determine test–retest reliability, and the results were found to be similar [Table I(A)].

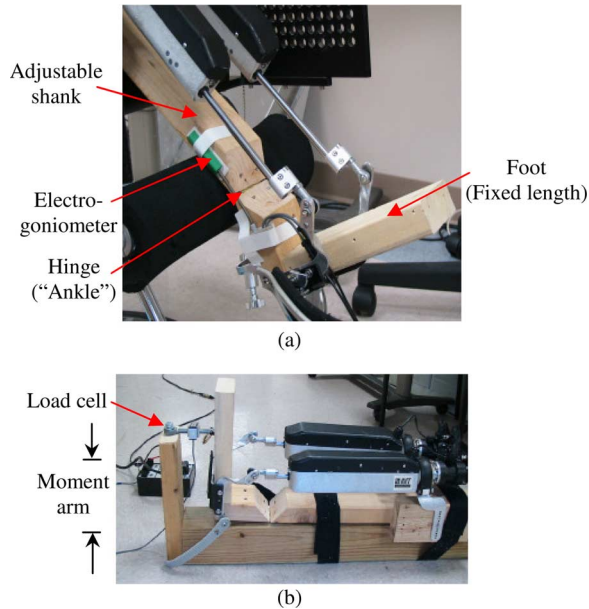


Fig. 6. Mock-up of shank, foot, and ankle joint with the Anklebot mounted on the mock-up undergoing. (Top) commanded displacement perturbations. An electrogoniometer is used to externally validate the accuracy of Anklebot's estimation of ankle kinematics; (bottom) undergoing isometric displacement perturbations. The load cell measures the linear force generated by the actuators. Tension and compression forces are generated by the Anklebot when the foot is commanded into dorsiflexion and plantarflexion, respectively.

D. Force/Torque Validation

The setup consisted of the ankle mock-up rigidly fixed to a wooden frame ("ground") in the horizontal position such that the "foot" was perpendicular to the "shank," i.e., "anatomical" neutral posture [Fig. 6(b)]. We commanded several ramp-and-hold displacements ("perturbations") in tension (dorsiflexion) and in compression (plantarflexion), all under isometric conditions. The actuator forces were measured using a load cell (MLP-200, Transducer Techniques, Temecula, CA) of maximum load 890 N and resolution 0.89 N. The load cell readings were compared against robot torques estimated by using motor commands and current sensor data.

Figure 7(b) shows the load cell readings, the commanded torque, and the motor current readings. Note that the region of interest, i.e., before torque saturation occurs with respect to commanded position, is between $\pm 15^\circ$ as the computer digital-to-analog board range is limited to ± 10 V. The software-invoked threshold at which torque saturation occurs is computed from the following expression:

$$\tau_{\text{clip}} = 2\varepsilon V_{\text{max}} r_{\text{trans}} \quad (4)$$

where τ_{clip} is the value of device torque above which clipping occurs, ε is a conversion factor from commanded voltage to device torque and equals 0.027 N·m/V for both the right and left motors, V_{max} is the voltage above which torque clipping occurs and is set at 10 V, and r_{trans} is the gear reduction or transmission ratio ~ 35 . Substituting the previous values in Eq. (4), we found that $\tau_{\text{clip}} = 19$ N·m [Table I(B)].

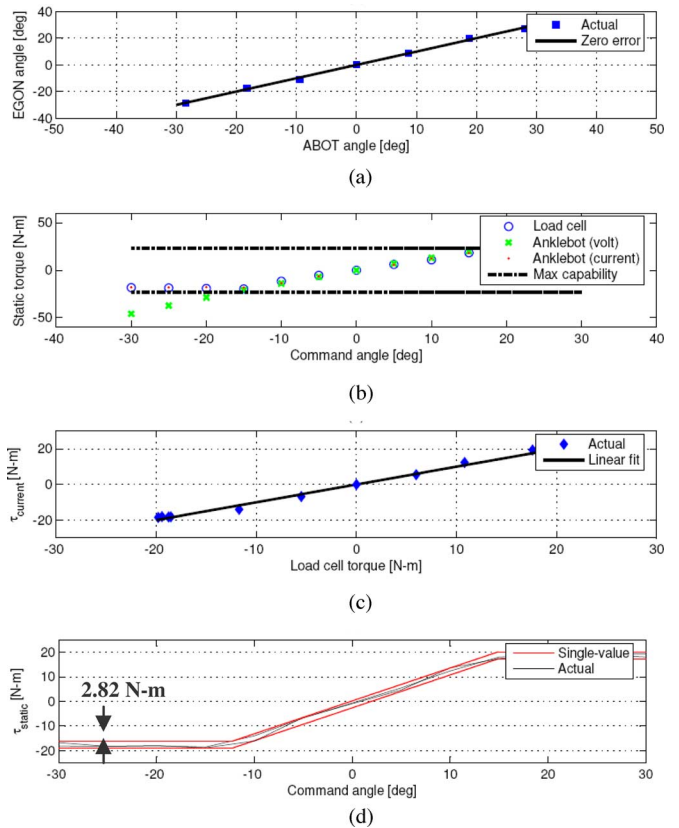


Fig. 7. (a) Anklebot angle estimates versus electrogoniometer (EGON) angle measurements plotted across the entire movement range tested. (b) Variation of torque estimated/measured using/by motor command voltage, current sensor, and load cell versus commanded perturbations. Negative and positive angles represent commanded plantarflexion (tension) and dorsiflexion (compression), respectively. The software-invoked saturation of current-based torque estimates can be clearly seen for perturbations greater than $\pm 15^\circ$. (c) Comparison of current-based torque estimates with load cell torques over the entire range of perturbations. (d) Uncertainty in torque estimates due to stiction. At any given perturbation, the estimated torque is bounded within the uncertainty region shown. A minimum-width single value of the uncertainty in torque is also shown (constant band).

The current-based torque estimate (τ_{current}) correlated strongly with the load cell measurements ($r^2 = 0.98$), with the mean absolute error across the entire range of commanded perturbations ($\pm 30^\circ$) between the two being less than 1 N·m. The magnitude of this error is equivalent to $< 2.5\%$ of the full torque range (FTR), i.e., the difference between maximum tension and maximum compression [Fig. 7(c)]. Further, the mean absolute errors in tension and compression were 2.27% and 3.06% of the FTR, respectively. Within the region of interest, the current- and voltage-based (τ_{volt}) torque estimates were strongly correlated ($r^2 = 0.99$), with a mean normalized error of 2.63%. These trends were highly repeatable across trials (mean normalized SD = 2.4%, 4%, and 3.6% for load cell, current- and voltage-based torques, respectively).

E. Static Friction

We found that when the actuator force (torque) was commanded to return to zero, it did not do so. The difference between

TABLE I
SUMMARY OF ANKLEBOT POSITION AND TORQUE VALIDATION

A. Position validation: regression and repeatability statistics				
Errors (deg) ^a (% Normalized ^c)		Correlation coefficient	P-value	Bias (deg) ^b
DF	PF			
0.75 (1.6)	0.89 (1.35)	99.61	1.75×10 ⁻⁶	0.86
Standard deviation (deg) ^d		Mean = 0.25, Max = 0.61		
B. Torque validation: saturation limits of current-based torque estimates versus predicted software clipping thresholds				
Measurement	Mean torque (N·m) for $\theta > 15^\circ$ (mean \pm SD)		FTR (N·m)	
	DF	PF		
Load cell	18.0 \pm 0.41	-18.9 \pm 0.45	38.2	
Current estimate	19.0 \pm 0.41	-18.1 \pm 0.11	37.9	
Software clip	Constant = 19		38.0	

^aErrors in dorsi- and plantarflexion refer to the mean absolute error.

^bBias is defined as the intercept of the least squares linear fit between electrogoniometer and Anklebot angle estimates.

^cErrors normalized to the full movement range measured by the electrogoniometer (55.6°).

^dStandard deviation was calculated for multiple measurements of Anklebot angle estimates. Means and maximum are reported for multiple measurements taken for the entire range of movement. DF: dorsiflexion, PF: plantarflexion, FTR: full torque range.

the initial and final nonactuated conditions provides a measure of static friction (or “stiction”), which was estimated using the following expression:

$$f_s^{(i)} = c\alpha_{\text{cal}} \left| v_{\infty, \text{no force}}^{(i)} - v_{0, \text{no force}}^{(i)} \right| \quad (5)$$

where superscript “*i*” refers to the value for the *i*th perturbation, f_s is the magnitude of stiction, c is the unit conversion factor (4.44 N/lbf), α_{cal} is the calibration constant of the load cell (24.9 lbf/V), $v_{\infty, \text{no force}}$ is the load cell voltage at final nonactuated condition, and $v_{0, \text{no force}}$ is the load cell voltage at initial nonactuated condition. The torque resulting due to stiction, which is normalized to the device FTR, is then given by

$$\tau_s^{(i)} = \frac{f_s^{(i)} R}{\max \tau_{\text{tension}} - \max \tau_{\text{compression}}} \quad (6)$$

where τ_s is the magnitude of torque due to stiction and R is the moment arm (24 cm), i.e., the vertical distance from the base of mock-up ankle to the point of attachment with the load cell.⁴

We found that the stiction averaged over the entire range of perturbations was 3.1 N, which corresponds to 0.744 N·m of torque due to stiction. This is less than 2% of the FTR and smaller than the resolution of the current-based torque estimates (2.46% FTR), supporting the idea that roughly 80% of estimate’s error arises from stiction. The uncertainty in torque estimation due to stiction depends on the commanded perturbation and is calculated as

$$\Delta_\tau^{(i)} = \tau^{(i)} - \varepsilon \tau_s^{(i)}, \quad 0 \leq \varepsilon \leq 1 \quad (7)$$

where Δ_τ is the uncertainty in torque due to stiction, τ is the current-based torque estimate, and $0 \leq \varepsilon \leq 1$ is a scalar representing the level of uncertainty. The uncertainty can be

⁴Note that since static friction is estimated under isometric conditions, the moment arm remains a constant for all commanded perturbations.

bounded by a minimum-width single-value band whose width is 2.82 N·m or 3.69% FTR [Fig. 7(d)].

F. Potential Confounding Effects

A number of potentially confounding factors were taken into account in the force/torque calibration of the device: first, the actuators are not exactly parallel to each other in the frontal plane, but instead, there exists a slight skew between them [Fig. 8(a)]. This affects the torque that is actually generated by the robot along the axis of the load cell as opposed to the torque estimated (which assumes no relative skew between the actuators). The skew was computed using device geometry and a correction factor included in our analysis:

$$\varphi = 2 \cos^{-1} \left(\frac{d_2 - d_1}{2l} \right), \quad \tau' = \tau \cos \left(\frac{\varphi}{2} \right) \quad (8)$$

where φ is the angle between the actuators, d_1 and d_2 are the vertical distances between the actuators at the two extremities, l is the rest length of actuators, and τ' and τ are the actual and estimated torques with and without skew correction, respectively. We found that the angle of skew was 9.05° so that the actual torque was 98.7% of the estimated torque.

Second, while it was ensured that actuators were approximately parallel to the load cell axis, any skew between the lines of action between the two can result in errors between the steady-state robot and load cell torques. This angle was computed using the following expression:

$$\theta = \frac{2d_1(l_1 - l_2)}{(l_2^2 - l_1^2 - d_2^2)}, \quad F_x = F \cos(\theta) \quad (9)$$

where θ is the angle between the lines of action of the load and actuator, F_x and F are the forces with and without skew correction, respectively, and $l_1, l_2, d_1,$ and d_2 are fixed geometric constants [Fig. 8(b)]. The angle of skew was found to be 5.6° so that the load cell torque was nearly 99.5% of the device torque. Finally, in order to assess the robustness of accuracy of torque estimation, the device was recalibrated in a “posture” other than the anatomical neutral. “Posture,” in this context, was characterized by the angular displacement of the ankle joint with respect to the vertical, i.e.,

$$\phi_{\text{max}} = \sin^{-1} \left(\frac{d_{\text{max}}}{l_f} \right), \quad \phi = n\phi_{\text{max}}, \quad F_{x'} = \frac{F_x}{\cos(\phi)} \quad (10)$$

where φ (or φ_{max}) is the angle (or maximum angle) measured from vertical, $F_{x'}$ and F_x are the forces along the anatomical (x - z) and rotated (x' - z') axes, respectively, $0 < n \leq 1$ is a user-defined constant defined as the ratio of the chosen angle to the maximum angle, and l_f and d_{max} are computed from geometry [Fig. 8(c)]. For example, at a “posture” of 18° ($\varphi_{\text{max}} = 45, n = 0.4$), we found that mean normalized error in torque was only 2% of the full force range capability of the device as opposed to an error of 2.46% for “posture” of 0°, i.e., anatomical neutral, thus suggesting that the accuracy of torque estimation is robust to ankle configuration.

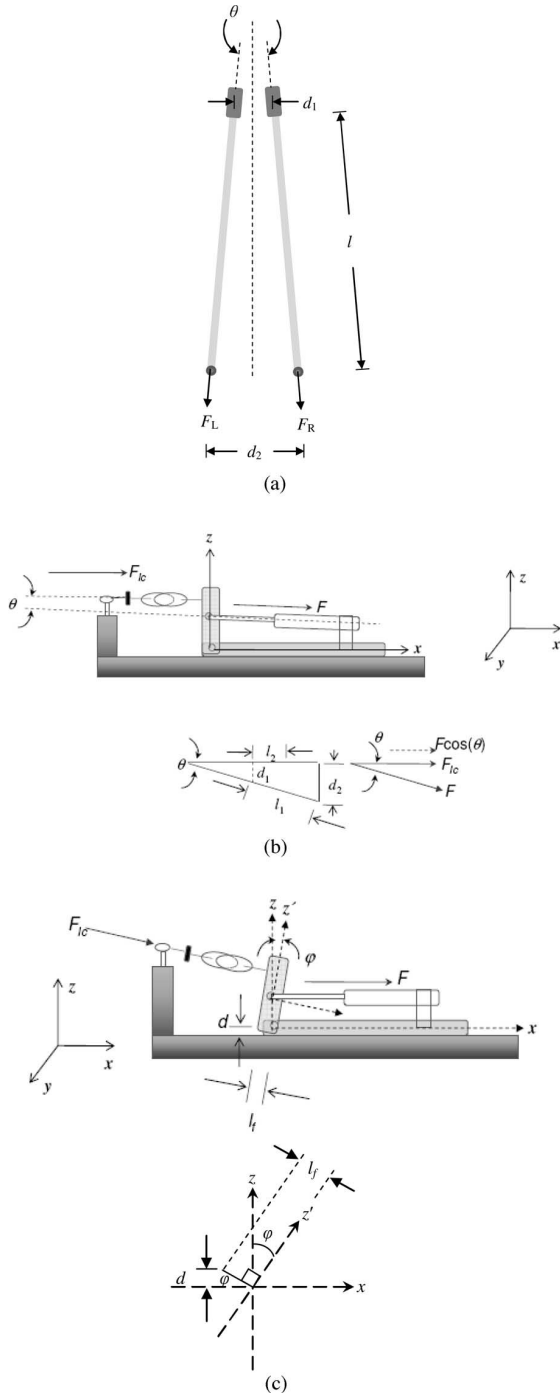


Fig. 8. Schematic showing confounding effects of Anklebot geometry on torque estimation. (a) Frontal view of the Anklebot showing the skew between the actuators. (b) Sagittal view showing angle between actuator and load cell axes. (c) Quantification of “posture” as characterized by angular displacement of mock-up ankle with respect to vertical.

V. EFFECTS OF UNILATERAL LOADING

Given that the current generation Anklebot weighs >3 kg, it is important to evaluate if the added mass on one limb significantly alters gait. Preliminary tests conducted with the first-generation (Alpha-I) prototype on unimpaired subjects [28] and stroke survivors have shown that gait characteristics during “free

TABLE II
EFFECT OF ANKLEBOT MASS ON SPATIOTEMPORAL GAIT PARAMETERS

Variable	Healthy ^a		Stroke ^a	
	WOM	WM	WOM	WM
Velocity ^b (m/s)	1.33 ^d (0.12)	1.29 (0.10)	0.49 (0.19)	0.44 (0.14)
Step time ^c (s)	0.58 (0.06)	0.61 (0.07)	0.89 (0.18)	0.96 (0.22)
Stance duration ^{c,e} (%)	63.9 (11.3)	63.2 (12.9)	60.3 (3.4)	59.3 (6.7)

^a $n = 5$ in each group.
^bOverground 24 ft walkway.
^cStep time and stance duration are for paretic (stroke) and dominant (healthy) limbs.
^dValues expressed and mean (SD).
^eExpressed as percent of heel strike to heel strike gait cycle. WOM: without mass, WM: with mass.

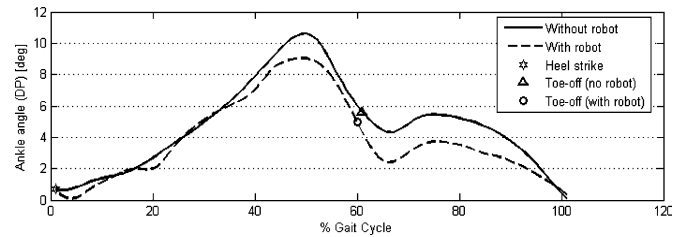


Fig. 9. Effects of unilateral loading. Paretic ankle position in dorsiflexion and plantarflexion in a single representative stroke subject during the gait cycle under two conditions (with and without robot mass). For comparison purposes, the start of swing phase (“toe-off”) is shown for both conditions.

walking,” asymmetric loading (robot on one leg), and symmetric loading (ankle robot on one leg and dummy mass on the other) were all comparable, indicating that the ankle robot does not interfere substantially with natural or impaired gait, which confirms a similar finding by Blaya and Herr [15]. We expanded on those initial studies with a series of tests conducted with the current prototype to assess how this unilateral loading would alter gait biomechanics. Healthy individuals ($n = 5$) and stroke survivors ($n = 5$) walked overground across an 8-m floor six times at a self-selected comfortable speed⁵ (Table II).

On a separate day, they walked on the treadmill for six trials that lasted 15 s each at a comfortable speed. During these tests, a 3-D motion analysis system (Optotrak Certus Motion Capture System, NDI, ON, Canada) was used to measure gait kinematics. Generally speaking, the spatiotemporal gait parameters (e.g., durations of stance and swing, ROM, etc.) were not significantly altered due to the added mass on the leg in most of the healthy and stroke subjects. Fig. 9 shows the ankle movement during overground gait for a representative stroke subject (female, 61.1 years, height = 1.64 m, mass = 61.8 kg, 7.4 years poststroke) under the two conditions (with (WM) and without (WOM) wearing the Anklebot—but with no robotic assistance). In this subject, the single stance (heel strike to toe-off time interval) and swing durations, which are expressed as a percentage of the gait cycle, were very similar between the two conditions overground (WM: stance $\sim 60.5\%$, swing $\sim 39.4\%$; WOM:

⁵All subjects gave their informed consent prior to testing. The protocol was approved by the MIT Committee on the Use of Humans as Experimental Subjects (MIT-COUHES), University of Maryland Institutional Review Board, and Baltimore Veterans Affairs Research and Development Committee.

stance $\sim 60.4\%$, swing $\sim 39.5\%$). Further, the maximum dorsiflexion (“toe-up”) decreased only marginally when the paretic limb was loaded (WM: 9.04° , WOM: 10.62°).

VI. EXAMPLE OF CLINICAL APPLICATION: ESTIMATION OF PASSIVE ANKLE STIFFNESS

A. Significance of Ankle Impedance

Ankle stiffness is a critical biomechanical factor in locomotion. Studies have shown that humans adjust leg stiffness to accommodate surface changes during hopping in place and forward running [30], [31], and there is evidence to suggest that modulation of ankle stiffness is the primary mechanism for adjusting leg stiffness under a variety of circumstances (e.g., [32]). Others have shown that the nondisabled human ankle appears to change stiffness characteristics as gait speed changes [33]. Further, there is evidence that adequate ankle joint stiffness is critical during the single support phase to control forward and downward body momentum [34]. Ankle impedance (i.e., stiffness plus damping and any other dynamic factors) is also important for the role it plays in “shock absorption,” in clearing the ground during the swing phase, and maintaining ankle stability during the stance phase. Ankle stability itself is influenced by passive mechanisms, e.g., ligamentous stiffness, as well as active mechanisms and neuromotor mechanisms such as reflex and voluntary control.

Despite extensive literature on the topic, there appears to be little consensus within the biomechanics or motor control communities about the accepted definition of terms such as *stiffness*. In the most general sense, *dynamic* impedance is a property of a system that maps the time history of displacement (or angle) onto the time history of force (or torque) and includes resistance to motion-related displacement, velocity, acceleration, and any other dynamic factors. In steady state, a linearized approximation relating steady displacement to steady force is characterized by a constant of proportionality known simply as stiffness. Stiffness can be categorized based on whether it is measured under passive or active conditions. *Passive* stiffness is measured at low speeds without subject’s intervention. It refers to the mechanical stiffness provided by the combination of the joint, tendon, and connective tissue [35]. The *intrinsic* joint stiffness is one that provides an immediate torque response to any change in joint angle without any intervention required from the nervous system [36] and, therefore, includes contribution from active muscle fibers in addition to mechanical properties of the joint and passive tissue. *Active* stiffness, on the other hand, is a function of muscle activation and reflex behavior. Active tension is generated when the muscle receives input at the neuromuscular junction (e.g., during a voluntary or reflexive contraction).

In neurologically impaired patients, spasticity (reflex hyperexcitability and hypertonus) might disrupt the remaining functional use of muscles [37]. It may be accompanied by structural changes of muscle fibers and connective tissue, which may result in alterations of intrinsic mechanical properties of a joint. Studies have shown, for example, that passive ankle stiffness in neurologically impaired individuals, e.g., those with spinal cord

injury (SCI) [38], spastic cerebral palsy (CP) [39], multiple sclerosis (MS) [40], or cerebral vascular accident (stroke) [37], [41], have abnormal passive ankle stiffness in addition to hypertonia. In other words, intrinsic properties of the ankle joint, such as passive stiffness, may be a potential signature of ankle pathology.

B. Theoretical Basis

A simple approach to estimate the passive static stiffness of the ankle using the Anklebot is to apply a series of nominally static displacements (reference or “target” angles) in a given DOF and measure the resultant angular displacements in that DOF. The total torque at the ankle is, in general, a vector sum of the human and robot torques. In this approach, the human torque component is minimized by instructing subjects to not intervene. Assuming minimal voluntary contribution, the total torque displacing the ankle can be considered to be approximately equal to the applied machine torque. Also, the bias torque, i.e., the torque output by the robot when no torque (or voltage) is commanded is negligible (7×10^{-4} N·m). Then, under these assumptions, the ratio of the ankle torque to angular displacement yields an estimate of the passive ankle stiffness under static conditions.

C. Experimental Paradigm

1) *Participants*: Study participants were ten healthy subjects (six men and four women) between 24 and 40 years of age (31 ± 6 years) of average dimensions (height: 167.3 ± 13.1 cm, mass: 61.5 ± 16.3 kg).

2) *Procedures*: All tests were performed with the subjects in a seated position with their knee flexed at 60° and ankle suspended [42]. Note that, in addition to the quick-release feature, all knee braces were modified to also include a potentiometer to measure knee angle. Subjects experienced a series of displacements of the ankle joint while in this position such that any translational movement of their knee was physically constrained (but knee flexion/extension was unconstrained). This avoided any confounding effects of knee movement during DP and/or IE. In all subjects, the right (self-reported dominant) ankle was tested. The anatomical neutral was taken as the “zero” position and was determined by positioning the foot on the ground at 90° with respect to the long axis of the leg. In order to minimize any contribution of voluntary “human” torque, subjects were instructed to “not intervene” when the perturbation occurred and keep their foot relaxed throughout [43].

The perturbations applied to the ankle joint were position-controlled constant velocity ramp-and-hold displacements (Fig. 10). Angles and torques in dorsiflexion and eversion were considered positive. Each perturbation was made at a constant velocity of $5^\circ/s$. These have been shown not to evoke reflex responses under similar experimental conditions [44]. Each perturbation was followed by a holding phase in the steady-state position lasting 1 s to obtain an artifact-free recording, which is an ankle version of the protocol used by Mussa-Ivaldi *et al.* in measuring arm postural stiffness [45].

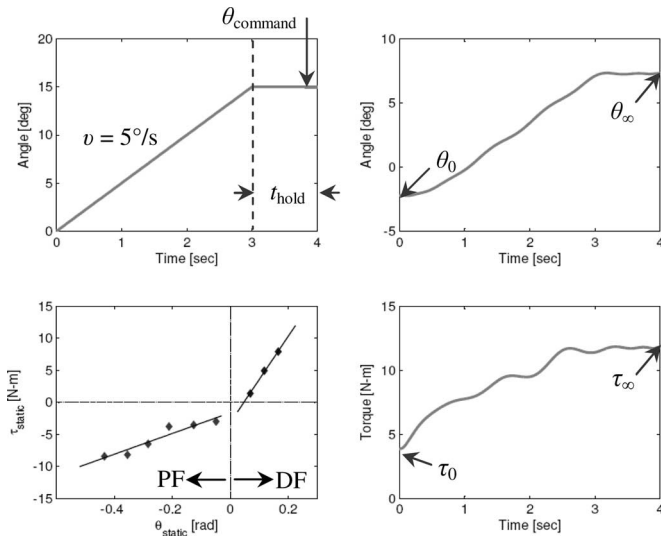


Fig. 10. Measurement of passive stiffness using the Anklebot. (a) Typical torque and angle data from a single subject. (Top left) Commanded ramp-and-hold displacement perturbation (θ_{command}) of 15° in dorsiflexion with constant velocity (v) of $5^\circ/\text{s}$ and hold time (t_{hold}) of 1 s; (top and bottom right) raw traces of ankle angle and torque for the same subject shown with initial (θ_0 , τ_0) and final conditions (θ_∞ , τ_∞); (bottom left) steady-state torque (τ_{static}) and angle (θ_{static}) data obtained by perturbing the subject's ankle over the entire range of commanded perturbations in the sagittal plane. Each data point is obtained by perturbing the ankle to a commanded angle and measuring the resultant net torque and angular displacement under static conditions. The slope of the linear regression line represents the passive ankle stiffness in a given direction. DF: dorsiflexion. PF: plantarflexion.

D. Results

Stiffness estimates were obtained using least squares linear regression. In each direction of movement, the neutral point was not included in the regression. The mapping between the static ankle torques and the resultant angular displacements across the entire range of movement was consistent across all subjects: 1) The estimates of passive ankle stiffness were dependent on the direction of ankle movement. In other words, the passive ankle stiffness averaged across all subjects was significantly different between dorsiflexion and plantarflexion ($P = 0.008$;⁶ see Fig. 11), and between eversion and inversion ($P = 0.003$); 2) the applied torque and ankle angle were significantly correlated in each direction within the range of commanded perturbations (dorsiflexion: $r^2 = 0.89 \pm 0.08$, $P \leq 0.07$, plantarflexion: $r^2 = 0.92 \pm 0.04$, $P \leq 0.08$, eversion: $r^2 = 0.93 \pm 0.05$, $P \leq 0.02$, inversion: $r^2 = 0.92 \pm 0.03$, $P \leq 0.08$) within the range of commanded perturbations justifying the use of least squares linear regression to estimate passive stiffness; and 3) the mean passive stiffness was significantly higher in dorsiflexion ($0.52 \pm 0.31 \text{ N}\cdot\text{m}/^\circ$) than in plantarflexion ($0.31 \pm 0.12 \text{ N}\cdot\text{m}/^\circ$), and significantly higher in eversion ($0.49 \pm 0.12 \text{ N}\cdot\text{m}/^\circ$) than in inversion ($0.34 \pm 0.05 \text{ N}\cdot\text{m}/^\circ$).

A number of factors had the potential to confound the fidelity of the data and were controlled as best as possible. They included: 1) variation in knee joint angle—since the knee angle has a strong influence on ankle stiffness (due to biarticular muscles

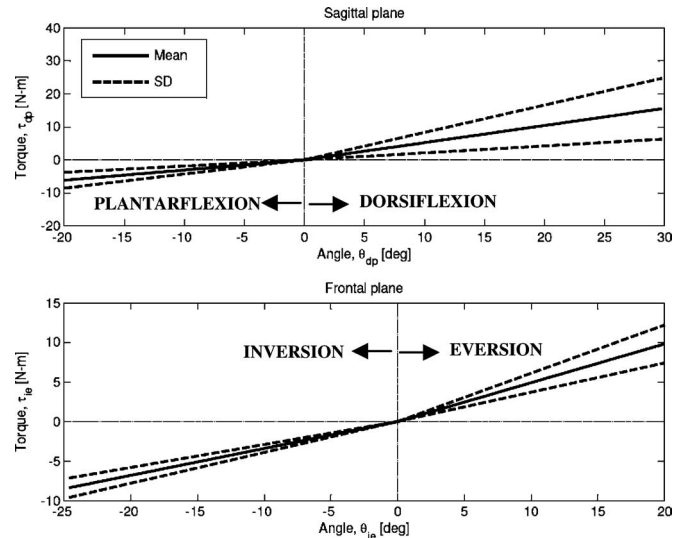


Fig. 11. Linear regressors of mean (dashed) \pm SD (solid) of passive stiffness estimates for all subjects in both the sagittal (top panel) and frontal (bottom panel) planes. Passive stiffness is estimated as the slope of the least squares linear regressor between applied torque τ (sagittal: τ_{dp} , frontal: τ_{ie}) and angular displacement θ (sagittal: θ_{dp} , frontal: θ_{ie}) with the offset value of machine torque subtracted. Separate regressors are computed to estimate ankle stiffness in each direction within a DOF. Dorsiflexion ($\theta > 0$)/plantarflexion ($\theta < 0$) in the sagittal plane and eversion ($\theta > 0$)/inversion ($\theta < 0$) in the frontal plane.

crossing the ankle and knee joints), we ensured that variation in knee angle was kept at a minimum. Variation of knee angle in flexion–extension was computed for each perturbation trial. The group average of flexion–extension (as measured from initial knee position 60°) was relatively “small” (maximum $\sim 1.7^\circ$ or 2.9% of the initial knee angle) in both planes of movement (sagittal plane: $0.09^\circ \pm 0.55^\circ$; frontal plane: $0.57^\circ \pm 1.15^\circ$). These variations are likely to be due to the subject's postural adjustments in between the perturbation trials and are unlikely to influence passive ankle stiffness; 2) in-shoe slippage—movement or slippage of the foot within the orthopedic shoe could confound the accuracy of kinematic and kinetic measurements; 3) movements not being truly passive—voluntary torque contribution could result in overestimation of passive stiffness. The “do-not-intervene” paradigm, in which the subject is asked not to react to the experimental changes, has been used in previous studies involving both the upper, e.g., arm [43] and wrist (e.g., [46]) as well as the lower extremity, e.g., lower leg [47], and has been found to be effective; 4) elicitation of stretch reflex—we used a slow perturbation velocity of $5^\circ/\text{s}$ to prevent elicitation of stretch reflex [44]; and 5) effects of gravity—overall, gravity had a negligible effect on passive ankle stiffness estimates. For example, the mean relative errors in passive stiffness estimates with and without gravity torques were less than 1% and 2.5% in dorsi- and plantarflexion, respectively.

E. Comparison With Published Literature

Few studies have reported data on young healthy individuals under similar conditions. Owing to similar experimental paradigms [Table III(A)], we compared our results with those obtained by: 1) Sinkjaer and others, who measured the

⁶Significance level was set at 0.05.

TABLE III
COMPARISON OF ANKLEBOT PROTOCOL AND STIFFNESS VALUES
WITH OTHER STUDIES

A. Various paradigms used to measure passive ankle stiffness			
Work/method	Posture	Mechanism	Perturbation characteristics
Anklebot^a		Passive robot forces	20° PF to 30° DF $v = 5^\circ/s$
Sinkjaer (1988)		Passive force plate rotations	2° DF, $v = 100^\circ/s$
Rydahl (2004)		Kin-Com dynamometer	5° DF, $v = 100^\circ/s$
Lamontagne (2000)	Seated, knee flexed	Custom-built intelligent stretching device	30° PF to PROM+5° DF, $v = 12-37^\circ/s$
Chung (2004)		Computer-controlled dynamometer	PROM in both DF/PF, Torque limit = 10 N-m
Singer (2002)		Custom-built dynamometer	DF stretches at PF moments (5 and 10 N-m)
Harlaar (2000)		Dynamometer	PF moment = 10 N-m
Zinder (2007)	Upright stance; full load bearing	Custom-built swaying cradle device	5° INV - 5° EV
Saripalli (2002)		Cradle platform and force plate	10° INV - 10° EV
B. Comparison of passive ankle stiffness estimates			
Criterion ^b	Published study	Passive stiffness ^c (N-m/deg ^d)	
Torque < 5 N-m (DF only)	Sinkjaer, 1988	1.17 ^e	
Perturbation = 5° (DF only)	Anklebot	0.54 ± 0.07	
	Rydahl, 2004	0.9 ± 0.44	
Full movement range (DF only)	Anklebot	0.46 ± 0.14	
	Lamontagne, 2000	0.3	
At 10° DF	Anklebot	0.2 ± 0.01	
	Chung, 2004	0.35 ± 0.20	
	Singer, 2002	0.44 ± 0.21	
At 30° PF	Harlaar, 2000	0.36 (0.32 - 0.47)	
	Anklebot	0.63 ± 0.15	
INV perturbations	Chung, 2004	0.13 ± 0.13	
	Anklebot	0.31 ± 0.12	
Full range of movement	Saripalli, 2002	~0.35-0.43 ^f	
	Anklebot	0.34 ± 0.05	
	Zinder, 2007	0.62 ± 0.16	
	Anklebot	0.41 ± 0.09	

^aAnklebot paradigm attributes and stiffness estimates are marked bold for comparison purposes.

^bThe methods used to measure passive ankle stiffness differed among the articles [see A].

^cValues are expressed as mean ± SD where available, or as mean (range).

^dValues are expressed in newtons meter per degree rather than newtons meter per radian to allow comparison between studies.

^eMean of maximum and minimum values of stiffness in 0-5 N-m range.

^fApproximate extrapolated range for 0% loading. DF: dorsiflexion, PF: plantarflexion, INV: inversion, EV: eversion, PROM: passive ROM, v: perturbation velocity.

intrinsic and reflex components of total stiffness in human ankle dorsiflexors [52]; 2) Rydahl and Brouwer, who estimated the passive ankle stiffness in healthy individuals and stroke survivors using a series of displacement perturbations in dorsiflexion [53]; 3) Lamontagne and others, who studied the contribution of passive stiffness to ankle plantarflexor moment during gait [54]; and 4) Chung and other, who investigated biomechanical changes in the passive properties (e.g., quasi-static stiffness in dorsiflexion and plantarflexion) in healthy and hemiplegic spastic ankles [37]. To the best of our knowledge, only two studies have measured passive ankle stiffness in the frontal plane: 1)

Saripalli and Wilson, who examined dynamic ankle stiffness and dynamic inversion stabilization as a function of ankle inversion and eversion with different levels of weight bearing [44], and 2) Zinder and colleagues, who tested the validity and reliability of a new measure of inversion-eversion ankle stiffness using a novel medial/lateral swaying cradle device [55]. Both those studies used healthy young subjects in an upright stance.

Our stiffness estimates are slightly 1) lower than those obtained for healthy individuals in [53] and [54]. This may be attributable to mean sample age differences in the healthy populations tested. These studies used age-matched controls against their neurologically impaired test population, whereas our study included young healthy subjects and 2) higher than those reported in [37] as well as other related studies [56], [57]. This could be due to the measurement of stiffness in different ROMs, which may or may not include the neutral. For example, Chung [37] reported lower passive quasi-stiffness in plantarflexion than that reported here possibly because they measured stiffness in a much wider ROM ($46.01^\circ \pm 9.65^\circ$) than used for our study ($16.16^\circ \pm 1.08^\circ$). Our frontal plane stiffness values were lower than those reported in [44] and [55]. We speculate that this might be due to the differences in postural and/or loading conditions under which stiffness was measured. For example, in [55], passive stiffness was measured with subjects in upright stance with full weight bearing condition. In [44], it was measured under upright stance with varying levels of body weight loading. They showed that passive stiffness increases with loading of the joint [43] and when extrapolated for 0% loading, their values are within the range of our inversion stiffness estimates (<0.1 N-m/° difference). These comparisons are summarized in Table III(B).

F. Qualitative Trends: Explanation Based on Muscle Physiology

One of our main findings is that passive ankle stiffness is dependent on the direction of movement. Such an observation has also been reported in [37] for the human ankle as well as in other anatomically similar joints, e.g., for wrist flexion-extension [48]. There is evidence to suggest that this dependence could be due to the summed physiologic cross-sectional area (SPCA) of the antagonist group of muscles undergoing passive stretch [49]. Assuming that the passive resistance to stretching is a main contributor to joint impedance [49] and that agonist muscles go slack during passive stretch, we believe that intrinsic stiffness of the ankle joint is directly related to the SPCA of the antagonist muscle group lengthened during passive stretch. If true, then we may explain the qualitative trends seen between torque and angle and, in particular, the direction dependence of passive ankle stiffness. We should expect to find that the SPCA of plantarflexors to be higher than that of dorsiflexors. Further, we also expect to find that the ratio of SPCA of plantar-to-dorsiflexors and that of invertors-to-evertors to be of the order of the ratio of passive stiffness in dorsi-to-plantarflexion and eversion-to-inversion, respectively.

In order to test the validity of our predictions, we used cadaver data and computed the SPCA of each group of physiologically

intact muscles that are dorsiflexors, plantarflexors, evertors, and invertors [50] and scaled these values with the square of mean moment arms of each group. Our findings were as follows: 1) As predicted, the SPCA of plantarflexors (83.36 cm^2) was greater than that of dorsiflexors (30.83 cm^2), and the SPCA of invertors (51.22 cm^2) was greater than that of evertors (30.38 cm^2); 2) the ratio of plantar-to-dorsiflexor and invertor-to-evertor SPCA with moment arm correction was 1.92 and 1.39, respectively. As predicted, these values are of the order of the mean value of dorsi-to-plantarflexion and eversion-to-inversion passive stiffness ratios of 1.72 and 1.43, respectively. In these calculations, we assumed that the muscle moment arm was invariant to passive stretch [51].

VII. CONCLUSION

This paper has presented the design and characterization of MIT's Anklebot, as well as its potential application as a clinical measurement tool to estimate ankle parameters such as passive stiffness. We are presently completing pilot studies with chronic stroke with very promising initial results. Preliminary findings already indicate that this device has the potential to evoke positive changes in gait function (e.g., walking speed), reduce impairments (e.g., passive ankle stiffness), and improve measures of motor control (e.g., smoothness of movement). Future studies would compare the efficacy of this device to more traditional "whole body" locomotor training programs, such as conventional and treadmill-based exercise programs. Ultimately, robotic technology would only undergo widespread adoption if it demonstrates to be both efficacious and effective, i.e., it provides additional benefits as compared to other therapies and it is cost-effective. We envision the Anklebot to facilitate insights into human motor recovery, gait, balance, and motor learning by providing a customizable, adaptive, and quantifiable measurement and rehabilitative tool.

ACKNOWLEDGMENT

Dr. H. I. Krebs and Dr. N. Hogan are coinventors in the MIT- and VA-held patent for the robotic device used in this paper. They hold equity positions in Interactive Motion Technologies, Inc., which is the company that manufactures this type of technology under license to MIT and VA. A. Roy thanks J. C. Mizelle, S. L. Patterson, T. N. Judkins, and I. Khanna for their help with the experiments.

REFERENCES

- [1] American Heart Assoc. (2009). Heart Disease and Stroke Statistics—2009 Update [Online]. Available: <http://www.americanheart.org/statistics>
- [2] R. J. Seitz, Y. Huang, U. Knorr, L. Tellmann, H. Herzog, and H. J. Freund, "Large-scale plasticity of the human motor cortex," *Neuroreport*, vol. 6, pp. 742–744, Mar. 1995.
- [3] M. Hallett, "Plasticity in the human motor system," *Neuroscientist*, vol. 5, pp. 324–332, Sep. 1999.
- [4] W. M. Jenkins and M. M. Merzenich, "Reorganization of neurocortical representations after brain injury: A neurophysiological model of the bases of recovery from stroke," *Progress Brain Res.*, vol. 71, pp. 249–266, 1987.
- [5] M. H. Schieber, "Physiological basis for functional recovery," *J. Neurol. Rehabil.*, vol. 9, pp. 65–71, Jan. 1995.
- [6] N. Hogan, H. I. Krebs, J. Charnnarong, P. Srikrishna, and A. Sharon, "MIT-MANUS: A workstation for manual therapy and training," in *Proc. Int. Workshop Robot Human Commun.*, Sep. 1992, pp. 161–165.
- [7] H. I. Krebs, B. T. Volpe, M. L. Aisen, and N. Hogan, "Increasing productivity and quality of care: Robot-aided neurorehabilitation," *VA J. Rehabil. Res. Dev.*, vol. 37, pp. 639–652, Nov./Dec. 2000.
- [8] B. T. Volpe, H. I. Krebs, N. Hogan, L. Edelstein, C. M. Diels, and M. L. Aisen, "Robot training enhanced motor outcome in patients with stroke maintained over 3 years," *Neurol.*, vol. 53, pp. 1874–1876, Jun. 1999.
- [9] B. T. Volpe, H. I. Krebs, N. Hogan, L. Edelstein, C. M. Diels, and M. L. Aisen, "A novel approach to stroke rehabilitation: Robot aided sensorimotor stimulation," *Neurol.*, vol. 54, pp. 1938–1944, May 2000.
- [10] B. T. Volpe, H. I. Krebs, and N. Hogan, "Is robot-aided sensorimotor training in stroke rehabilitation a realistic option?" *Curr. Opin. Neurol.*, vol. 14, pp. 745–752, Dec. 2001.
- [11] M. Ferraro, J. J. Palazzolo, J. Krol, H. I. Krebs, N. Hogan, and B. T. Volpe, "Robot aided sensorimotor arm training improves outcome in patients with chronic stroke," *Neurol.*, vol. 61, pp. 1604–1607, Dec. 2003.
- [12] S. Fasoli, H. I. Krebs, J. Stein, W. R. Frontera, and N. Hogan, "Effects of robotic therapy on motor impairment and recovery in chronic stroke," *Arch. Phys. Med. Rehabil.*, vol. 84, pp. 477–482, Apr. 2003.
- [13] S. Fasoli, H. I. Krebs, J. Stein, W. R. Frontera, R. Hughes, and N. Hogan, "Robotic therapy for chronic motor impairments after stroke: Follow-up results," *Arch. Phys. Med. Rehabil.*, vol. 85, pp. 1106–1111, Jul. 2004.
- [14] J. Stein, H. I. Krebs, W. R. Frontera, S. E. Fasoli, R. Hughes, and N. Hogan, "Comparison of two techniques of robot-aided upper limb exercise training after stroke," *Amer. J. Phys. Med. Rehabil.*, vol. 83, pp. 720–728, Sep. 2004.
- [15] H. I. Krebs and N. Hogan, "Therapeutic robotics: A technology push," *Proc. IEEE*, vol. 94, no. 9, pp. 1727–1738, Sep. 2006.
- [16] J. A. Blaya and H. Herr, "Adaptive control of a variable-impedance ankle-foot orthosis to assist drop-foot gait," *IEEE Trans. Neural Syst. Rehabil. Eng.*, vol. 12, no. 1, pp. 24–31, Mar. 2004.
- [17] S. J. Brown, *Marketing Trends in Managed Care*. Dallas, TX: Baylor Inst. Rehabil., 1995.
- [18] W. E. Carlsson, C. L. Vaughan, D. L. Damiano, and M. F. Abel, "Orthotic management of gait in spastic diplegia," *Amer. J. Phys. Med. Rehabil.*, vol. 76, pp. 219–225, May/June 1997.
- [19] S. Hesse and D. Uhlenbrock, "A mechanized gait trainer for restoration of gait," *J. Rehabil. Res. Dev.*, vol. 37, pp. 701–708, Nov./Dec. 2000.
- [20] D. P. Ferris, J. M. Czerniecki, and B. Hannaford, "An ankle-foot orthosis powered by artificial pneumatic muscles," *J. Appl. Biomech.*, vol. 21, pp. 189–197, May 2005.
- [21] J. B. Andersen and T. Sinkjaer, "An actuator system for investigating electrophysiological and biomechanical features around the human ankle joint during gait," *IEEE Trans. Rehabil. Eng.*, vol. 3, no. 4, pp. 299–306, Dec. 1995.
- [22] M. Girone, G. Burdea, M. Bouzit, and V. Popescu, "A Stewart platform-based system for ankle telerehabilitation," *Auton. Robots*, vol. 10, pp. 203–212, Mar. 2001.
- [23] G. Colombo, M. Jörg, R. Schreier, and V. Dietz, "Treadmill training of paraplegic patients using a robotic orthosis," *J. Rehabil. Res. Dev.*, vol. 37, pp. 693–700, Nov./Dec. 2000.
- [24] M. Pohl, C. Werner, M. Holzgräfe, G. Kroczeck, J. Mehrholz, I. Wingendorf, G. Hölig, R. Koch, and S. Hesse, "Repetitive locomotor training and physiotherapy improve walking and basic activities of daily living after stroke: A single-blind, randomized multicentre trial (Deutsche GAngrainerstudie: DEGAS)," *Clin. Rehabil.*, vol. 21, pp. 17–27, Jan. 2007.
- [25] J. Mehrholz, C. Werner, J. Kugler, and M. Pohl, "Electromechanical-assisted training for walking after stroke," *Cochrane Database Systematic Reviews*, no. 4, pp. 5–8, 2007 (art. no.: CD006185, doi: 10.1002/14651858.CD006185.pub2).
- [26] L.-Q. Zhang, S. G. Chung, Z. Bai, D. Xu, E. M. Rey, M. W. Rogers, M. E. Johnson, and E. J. Roth, "Intelligent stretching of ankle joints with contracture/spasticity," *IEEE Trans. Neural Syst. Rehabil. Eng.*, vol. 10, no. 3, pp. 149–157, Sep. 2002.
- [27] K. Bharadwaj, T. G. Sugar, J. B. Koeneman, and E. J. Koeneman, "Design of a robotic gait trainer using spring over muscle actuators for ankle stroke rehabilitation," *ASME Trans. Biomech. Eng.*, vol. 127, pp. 1009–1013, Nov. 2005.
- [28] J. W. Wheeler, H. I. Krebs, and N. Hogan, "An ankle robot for a modular gait rehabilitation system," in *Proc. IEEE/RSJ Intel. Robots Syst.*, 2004, vol. 2, pp. 1680–1684.

- [29] J. Perry, *Gait Analysis: Normal and Pathologic Function*. Thorofare, NJ: Slack, 1992.
- [30] D. P. Ferris and C. T. Farley, "Interaction of leg stiffness and surface stiffness during human hopping," *J. Appl. Physiol.*, vol. 82, pp. 15–22, Jan. 1997.
- [31] D. P. Ferris, M. Louie, and C. T. Farley, "Running in the real world: Adjusting leg stiffness for different surfaces," *Proc. R. Soc. B*, vol. 265, pp. 989–994, Jan. 1998.
- [32] C. T. Farley, H. P. Houdijk, C. van Strien, and M. Louie, "Mechanism of leg stiffness adjustment for hopping on surfaces of different stiffnesses," *J. Appl. Physiol.*, vol. 85, pp. 1044–1055, Sep. 1998.
- [33] A. H. Hansen, D. S. Childress, S. C. Miff, S. A. Gard, and K. P. Mesplay, "The human ankle during walking: Implications for design of biomimetic ankle prostheses," *J. Biomech.*, vol. 37, pp. 1467–1474, Oct. 2004.
- [34] S. D. Lark, J. G. Buckley, S. Bennett, D. Jones, and A. J. Sargeant, "Joint torques and dynamic joint stiffness in elderly and young men during stepping down," *Clin. Biomech.*, vol. 18, pp. 848–855, Nov. 2003.
- [35] G. B. Salsich, M. J. Mueller, and S. A. Sahrman, "Passive ankle stiffness in subjects with diabetes and peripheral neuropathy versus an age-matched comparison group," *Phys. Therapy*, vol. 80, pp. 352–362, Apr. 2000.
- [36] I. D. Loram and M. Lakie, "Direct measurement of human ankle stiffness during quiet standing: The intrinsic mechanical stiffness is insufficient for stability," *J. Physiol.*, vol. 545, pp. 1041–1053, Dec. 2002.
- [37] S. G. Chung, E. Rey, Z. Bai, E. J. Roth, and L.-Q. Zhang, "Biomechanic changes in passive properties of hemiplegic ankles with spastic hypertonia," *Arch. Phys. Med. Rehabil.*, vol. 85, pp. 1638–1646, Oct. 2004.
- [38] M. M. Mirbagheri, H. Barbeau, M. Ladouceur, and R. E. Kearney, "Intrinsic and reflex stiffness in normal and spastic, spinal cord injured subjects," *Exp. Brain Res.*, vol. 141, pp. 446–459, Dec. 2001.
- [39] R. L. Lieber and J. Friden, "Spasticity causes a fundamental rearrangement of muscle-joint interaction," *Muscle Nerve*, vol. 25, pp. 265–270, Jan. 2002.
- [40] L.-Q. Zhang, T. Nishida, G. Wang, J. Sliwa, D. Xu, and W. Z. Rymer, "Measures and mechanisms of hyperactive tendon reflexes in spastic multiple sclerosis patients," *Arch. Phys. Med. Rehabil.*, vol. 81, pp. 901–909, Jul. 2000.
- [41] S. G. Chung, E. van Rey, Z. Bai, W. Z. Rymer, E. J. Roth, and L. Q. Zhang, "Separate quantification of reflex and nonreflex components of spastic hypertonia in chronic hemiparesis," *Arch. Phys. Med. Rehabil.*, vol. 89, pp. 700–710, Apr. 2008.
- [42] A. Roy, H. I. Krebs, S. L. Patterson, T. N. Judkins, I. Khanna, L. W. Forrester, R. M. Macko, and N. Hogan, "Measurement of human ankle stiffness using the Anklebot," in *Proc. IEEE 10th Int. Conf. Rehabil. Robot.*, Jun. 2007, vol. 1, pp. 356–363.
- [43] J. J. Palazzolo, M. Ferraro, H. I. Krebs, D. Lynch, B. T. Volpe, and N. Hogan, "Stochastic estimation of arm mechanical impedance during robotic stroke rehabilitation," *IEEE Trans. Neural Syst. Rehabil. Eng.*, vol. 15, no. 1, pp. 94–103, Mar. 2007.
- [44] A. Saripalli and S. Wilson, "Dynamic ankle stability and ankle orientation," presented at the 7th Symp. Footwear Biomech. Conf., Cleveland, OH, Jul. 2005.
- [45] F. A. Mussa Ivaldi, N. Hogan, and E. Bizzi, "Neural, mechanical, and geometric factors subserving arm posture in humans," *J. Neurosci.*, vol. 5, pp. 2732–2743, Oct. 1985.
- [46] H. Moritomo, T. Murase, A. Goto, K. Oka, K. Sugamoto, and H. Yoshikawa, "In vivo three-dimensional kinematics of the midcarpal joint of the wrist," *J. Bone Joint Surg. (Amer.)*, vol. 88, pp. 611–621, Mar. 2006.
- [47] A. D. Walshe, G. J. Wilson, and A. J. Murphy, "The validity and reliability of a test of lower body musculotendinous stiffness," *Eur. J. Appl. Phys.*, vol. 73, pp. 332–339, May 1996.
- [48] N. Rijnveld and H. I. Krebs, "Passive wrist joint impedance in flexion—Extension and abduction—Adduction," in *Proc. IEEE 10th Int. Conf. Rehabil. Robot.*, Jun. 2007, vol. 1, pp. 43–47.
- [49] R. V. Gonzalez, T. S. Buchanan, and S. L. Delp, "How muscle architecture and moment arms affect wrist flexion—Extension moments," *J. Biomech.*, vol. 30, pp. 705–712, Jul. 1997.
- [50] G. T. Yamaguchi, A. G. U. Sawa, D. W. Moran, M. J. Fessler, and J. M. Winters, "A survey of human musculotendon actuator parameters," in *Multiple Muscle Systems*, J. M. Winters and S. L. Woo, Eds. New York: Springer-Verlag, 1990, pp. 717–774.
- [51] J. Hicks, A. Arnold, F. Anderson, M. Schwartz, and S. Delp, "The effect of excessive tibial torsion on the capacity of muscles to extend the hip and knee during single-limb stance," *Gait Posture*, vol. 26, pp. 546–552, Oct. 2007.
- [52] T. Sinkjaer, E. Toft, S. Andreassen, and B. C. Honemann, "Muscle stiffness in human ankle dorsiflexors: Intrinsic and reflex components," *J. Neurophysiol.*, vol. 60, pp. 1110–1121, Sep. 1988.
- [53] S. J. Rydahl and B. J. Brouwer, "Ankle stiffness and tissue compliance in stroke survivors: A validation of myotonometer measurements," *Arch. Phys. Med. Rehabil.*, vol. 85, pp. 1631–1637, Oct. 2004.
- [54] A. Lamontagne, F. Malouin, and C. L. Richards, "Viscoelastic behavior of plantar flexor muscle-tendon unit at rest," *J. Orthop. Sports Phys. Therapy*, vol. 26, pp. 244–252, Nov. 1997.
- [55] S. M. Zinder, K. P. Granata, D. A. Papua, and B. M. Gansneder, "Validity and reliability of a new in vivo ankle measurement device," *J. Biomech.*, vol. 40, pp. 463–467, Feb. 2007.
- [56] B. Singer, J. Dunne, K. Singer, and G. Allison, "Evaluation of triceps surae muscle length and resistance to passive lengthening in patients with acquired brain injury," *Clin. Biomech. (Bristol Avon)*, vol. 17, pp. 151–161, Feb. 2002.
- [57] J. Harlaar, J. Becher, C. Snijders, and G. Lankhorst, "Passive stiffness characteristics of ankle plantar flexors in hemiplegia," *Clin. Biomech. (Bristol Avon)*, vol. 15, pp. 261–270, May 2000.



Anindo Roy (M'04) received the B.Tech. degree from Jamia Millia Islamia University, New Delhi, India, in 1998, the M.Phil. degree in control systems engineering from the University of Sussex, Brighton, U.K., in 2000, and the Ph.D. degree in applied science (option engineering science and systems) from the University of Arkansas, Little Rock, in 2005.

From 2005 to 2006, he was a Postdoctoral Research Fellow with the Department of Biomedical Engineering, Georgia Institute of Technology, Atlanta. In 2006, he joined the Department of Mechanical Engineering, Massachusetts Institute of Technology (MIT), Cambridge, where he is currently a Postdoctoral Associate with the Newman Laboratory for Biomechanics and Human Rehabilitation. At MIT, his research has focused on the application of ankle robotics in stroke rehabilitation, specifically, using robotics as clinical measurement instruments and developing robot-assisted gait algorithms for chronic stroke survivors. He is also a Research Fellow at Baltimore Veterans Affairs Medical Center, Baltimore, MD. He has authored or coauthored more than 20 scientific articles on high-impact peer-reviewed journals and conference proceedings. His current research interests include biomechanics, biological control systems, rehabilitation robotics, motor control, and neurophysiology.



Hermano Igo Krebs (M'96–SM'06) received the Electrician degree from the Escola Tecnica Federal de Sao Paulo, Sao Paulo, Brazil, in 1976, the B.S. and M.S. degrees in naval engineering (option electrical) from the University of Sao Paulo, in 1980 and 1987, respectively, the M.S. degree in ocean engineering from Yokohama National University, Yokohama, Japan, in 1989, and the Ph.D. degree in engineering from Massachusetts Institute of Technology (MIT), Cambridge, in 1997.

In 1997, he joined the Department of Mechanical Engineering, MIT, where he is currently a Principal Research Scientist and a Lecturer at Newman Laboratory for Biomechanics and Human Rehabilitation. He is also an Adjunct Professor with the Department of Neurology, University of Maryland School of Medicine, Baltimore. He is also an Adjunct Research Professor of neuroscience at Weill Medical College, Cornell University, White Plains, NY. He is one of the founders of Interactive Motion Technologies: a Massachusetts-based start-up company commercializing robot technology for rehabilitation. From 1977 to 1978, he taught electrical design at the Escola Tecnica Federal de Sao Paulo. From 1978 to 1979, he was with the University of Sao Paulo in a project involving the identification of hydrodynamic coefficients during ship maneuvers. From 1980 to 1986, he was a Surveyor of ships, offshore platforms, and container cranes at the American Bureau of Shipping, Sao Paulo office. In 1989, he was a Visiting Researcher at Sumitomo Heavy Industries, Hiratsuka Laboratories, Japan. From 1993 to 1996, he was with Casper, Phillips, and Associates, where he worked on container cranes and control systems. He is involved in revolutionizing the way rehabilitation medicine is practiced today by applying robotics and information technology to assist, enhance, and quantify rehabilitation, particularly, neurorehabilitation. His current research interests include neurorehabilitation, functional imaging, human-machine interactions, robotics, and dynamic systems modeling and control.



Dustin J. Williams received the B.S. degree (*summa cum laude*) in mechanical engineering from the University of California, Los Angeles, and the M.S. degree in mechanical engineering from Massachusetts Institute of Technology, Cambridge.

He was a Research and Development Engineer for intuitive surgical for 2 years, where he developed a new line of endowrist instruments. From 2003 to 2007, he was a Research and Development Engineer at Interactive Motion Technologies, Cambridge, where he was involved in the field of ankle, shoulder/elbow, wrist, hand, and antigravity machines and was promoted to the Director of Operations/Engineering in 2007.

He is currently Professor with the Departments of Neurology, Medicine, and Physical Therapy and Rehabilitation Sciences, the Director of the Department of Veteran's Affairs Rehabilitation Research and Development Center of Excellence in Exercise and Robotics, the Associate Director of Research for the Geriatric Research Education and Clinical Core at the Baltimore Veterans Affairs Medical Center. He is the Academic Director of the University of Maryland School of Medicine Rehabilitation Medicine Division and a Standing Member of the Center for Medical Rehabilitation Research Grants Panel (National Institute of Child Health and Human Development) and VA Rehabilitation Research Grant Panels. His current interests include developing models of task-oriented exercise to improve motor function and cardiovascular fitness and metabolic health for individuals aging with the chronic disability of stroke. He has conducted studies of exercise-mediated neuromuscular adaptations at the central nervous system and peripheral muscular/metabolic levels to improve ambulatory function in older hemiparetic stroke patients and has also conducted studies of lower extremity ankle robotic-assistive devices for stroke rehabilitation over the past four years.



Christopher T. Bever received the B.A. degree from Washington University in Saint Louis, Saint Louis, MO, in 1971, the M.D. degree from the University of Rochester, Rochester, NY, in 1975, and the M.B.A. degree from Johns Hopkins University, Baltimore, MD, in 2005.

He completed a residency in internal medicine at Rutgers-College of Medicine and Dentistry of New Jersey, Piscataway, NJ, in 1977, a residency in neurology with Columbia-Presbyterian Medical Center, New York, in 1980, and fellowship training in immunology and neuroimmunology with the National Institutes of Health in 1984.

Since 1987, he has been on the faculty of the University of Maryland School of Medicine, Baltimore, where he is currently a Professor with the Departments of Neurology, Pharmacology, and Experimental Therapeutics and Physical Therapy and Rehabilitation Sciences, an Associate Chief of Staff for Research and Development at Baltimore Veterans Affairs Medical Center, the Director of the Department of Veteran's Affairs Multiple Sclerosis Center of Excellence-East, and the Co-Director of the VA Rehabilitation Research and Development Service Center on Exercise Training and Robotics. His current research interests include laboratory and clinical studies of new therapeutic approaches to the treatment of multiple sclerosis. He has conducted studies of disease-modifying therapies as well as the measurement of impairment and symptomatic treatment of neurologically impaired patients. He has also conducted studies of robotic-assistive devices for rehabilitation over the past eight years.



Larry W. Forrester received the A.B. degree in psychology from Duke University, Durham, NC, in 1972, the M.A. degree in physical education from Wake Forest University, Winston-Salem, NC, in 1984, and the Ph.D. degree from the University of Maryland, College Park, in 1997.

He completed postdoctoral fellowship training in stroke rehabilitation at Baltimore Veterans Affairs Medical Center (VAMC), Baltimore, MD, in 1999. Since 1999, he has been with the faculty of the University of Maryland School of Medicine,

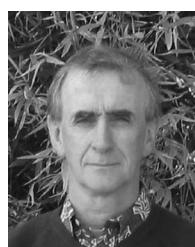
Baltimore, where he is currently an Associate Professor with the Departments of Physical Therapy and Rehabilitation Science and Neurology and a Research Fellow in geriatric rehabilitation at Baltimore VAMC, where he is also the Director of the Human Motor Performance Laboratory. His current research interests include neurorehabilitation after stroke, with an emphasis on exercise and motor-learning-based approaches that promote central nervous system plasticity. He is currently funded through the VA Rehabilitation Research and Development Service and the University of Maryland Claude D. Pepper Older Americans Independence Center to implement lower extremity robotics applications aimed at restoring mobility and balance functions in stroke survivors with hemiparesis. During the study of task-oriented treadmill training, he has investigated both the functional outcomes and the associated neuromuscular mechanisms of recovery through applications of biomechanics, transcranial magnetic stimulation, functional magnetic resonance imaging, and electroencephalography.



Richard M. Macko received the B.S. degree from Hiram College, Hiram, OH, in 1979 and the M.D. degree from Ohio State University, Columbus, in 1987.

He completed an internship at Riverside Methodist Hospital, Columbus, in 1988, a residency in neurology at the University of California at Los Angeles in 1991, and fellowship training in stroke rehabilitation at the University of Southern California, Los Angeles, in 1993. Since 1993, he has been with the faculty of the University of Maryland School of Medicine, Baltimore, where he

is currently Professor with the Departments of Neurology, Medicine, and Physical Therapy and Rehabilitation Sciences, the Director of the Department of Veteran's Affairs Rehabilitation Research and Development Center of Excellence in Exercise and Robotics, the Associate Director of Research for the Geriatric Research Education and Clinical Core at the Baltimore Veterans Affairs Medical Center. He is the Academic Director of the University of Maryland School of Medicine Rehabilitation Medicine Division and a Standing Member of the Center for Medical Rehabilitation Research Grants Panel (National Institute of Child Health and Human Development) and VA Rehabilitation Research Grant Panels. His current interests include developing models of task-oriented exercise to improve motor function and cardiovascular fitness and metabolic health for individuals aging with the chronic disability of stroke. He has conducted studies of exercise-mediated neuromuscular adaptations at the central nervous system and peripheral muscular/metabolic levels to improve ambulatory function in older hemiparetic stroke patients and has also conducted studies of lower extremity ankle robotic-assistive devices for stroke rehabilitation over the past four years.



Neville Hogan received the Dip. Eng. degree (with distinction) from Dublin Institute of Technology, Dublin, Ireland, and the M.S., M.E., and Ph.D. degrees from Massachusetts Institute of Technology (MIT), Cambridge.

In 1979, he joined the School of Engineering, MIT, where he was the Head and the Associate Head of the MIT Mechanical Engineering Department's System Dynamics and Control Division and is currently a Professor of mechanical engineering and a Professor of brain and cognitive sciences and the Director of

the Newman Laboratory for Biomechanics and Human Rehabilitation. He is a Founder and the Director of Interactive Motion Technologies, Inc. His current research interests include motor neuroscience, rehabilitation engineering, and robotics.

Prof. Hogan has been awarded Honorary Doctorates from Delft University of Technology and Dublin Institute of Technology, the Silver Medal of the Royal Academy of Medicine in Ireland, and the Henry M. Paynter Outstanding Investigator Award from the Dynamic Systems and Control Division, American Society of Mechanical Engineers.